Available online at www.sciencedirect.com
SCIENCE DIRECT®
Optics Communications 220 (2003) 289–295
OPTICS COMMUNICATIONS
www.elsevier.com/locate/optcom

Holographic grating recorded by He–Ne laser operating at 632.8 nm in polymer film containing push–pull azo dye

Yanjie Zhang[a,1], Zifeng Lu[b], Xuefeng Deng[b], Yichun Liu[a,b,*], Yingying Zhao[c]

[a] *Key Laboratory of Excited State Process, Changchun Institute of Optics, Fine Mechanics and Physics, Chinese Academy of Sciences, Changchun 130021, PR China*
[b] *Institute of Theoretical Physics, Northeast Normal University, Changchun 130024, PR China*
[c] *Department of Chemistry, Jilin University, Changchun 130023, PR China*

Received 12 March 2003; received in revised form 12 March 2003; accepted 8 April 2003

Abstract

Holographic gratings were optically recorded by two beams from a He–Ne laser operating at 632.8 nm in poly (methyl methacrylate) (PMMA) film containing push–pull azo dye. The holographic characteristics of the recorded gratings were dependent on the polarization direction of the recording beams and the relationship between the diffractive signals and the power density of recording beams was investigated. The formation of holographic gratings accompanied by 532 nm (double-frequency of Nd:YAG laser) irradiation was studied in detail. It was found that the effect of 532 nm laser to the holographic grating lay in two aspects. The acceleration effect of 532 nm laser to the formation of holographic grating is predominant when the power density of 532 nm laser is low. While at relatively high power density of 532 nm laser, the erasure is the main factor to the holographic grating. Moreover, the holographic grating was probed by 532 nm laser at low power density and the dependence of the first order diffractive signal on the recording beam power density was also presented.

Keywords: Holographic grating; He–Ne laser; Push–pull azo dye; 532 nm laser irradiation

1. Introduction

Azobenzenes with both electron donor (D) and acceptor (A) have attracted considerable attention due to their second-order nonlinear optical effect and polarized light-induced anisotropy [1–8]. This push–pull type of azo dyes has a large polarity than that of azobenzene without a substituent, and the *cis* molecules of push–pull azobenzenes formed via the photoisomerization process can thermally reisomerize to the *trans* molecules quickly because of large charge separation induced by D and A [1,7]. This kind of azo dyes has red-shifted absorption than those without substituents, which makes it possible to perform optical storage by

* Corresponding author. Tel.: +979-845-7638; fax: +979-845-7561.
E-mail address: ycliu@nenu.edu.cn (Y. Liu).
[1] Current address: Department of Chemistry, Texas A&M University, College Station, TX 77843-3255, USA.

0030-4018/03/$ - see front matter
doi:10.1016/S0030-4018(03)01420-2

polarized red waveband laser as writing beam. Previously, most studies of optical information storage focus on the Ar laser (488 or 514.5 nm) and double-frequency of Nd:YAG laser (532 nm) acting as writing beams [5–15]. Optical storage can also be accomplished by the 632.8 nm line of a He–Ne laser for methyl orange doped polyvinyl alcohol films preirradiated by a Ar laser [16,17]. However, little attention has been drawn on the optical storage of azo materials performed by polarized red waveband laser, such as He–Ne laser directly.

In present work, holographic gratings were optically recorded by He–Ne laser of 632.8 nm in poly (methyl methacrylate) (PMMA) film containing a kind of azo dye with both electron donor and acceptor. The formation of holographic grating accompanied by 532 nm irradiation was investigated in detail. The optical information storage performed by red waveband laser would be a significant interest because of the availability of semiconductor lasers.

2. Materials and UV–Vis spectra

The chemical structures of 4-[*N*-(2-hydroxyethyl)-*N*-methyl]amino-4′-nitroazobenzene (AZO-1) in *trans* and *cis* configurations are shown in Fig. 1. Commercially available (PMMA) is used without further purification. Both AZO-1 and PMMA are dissolved in $CHCl_3$ and then cast on a clean glass substrate. After the solvent evaporated slowly, the composite film is used for the measurements of holographic recording. The dye

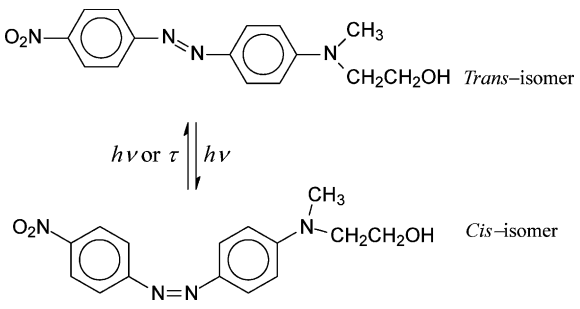

Fig. 1. Chemical structure of AZO-1 with *trans* and *cis* configurations.

concentration is set to be 1.0 wt% and the thickness of the film is about 10 μm.

The UV–Vis spectra are carried out using a Shimadzu-1600 spectrometer. The UV–Vis spectrum of AZO-1 doped PMMA film is shown as Fig. 2(a). It manifests one characteristic spectral band at 490 nm corresponds to π–π^* electronic transition in the *trans*-isomer of azo-chromophore. AZO-1 has both electron donor and acceptor attached to the benzene rings. This push–pull type of azo molecules has a large polarity than that of an azobenzene without a substituent. The *cis* isomer of push–pull azobenzenes formed via the photoisomerization process can return to the *trans* molecule quickly by thermal reisomerization [1,7]. So the n–π^* electronic transition for *cis* isomer cannot be detected in AZO-1 doped PMMA film. The large polarity and the fast reisomerization (thermal isomerization) lead push–pull azo molecules towards becoming prospective optical materials utilizing the polarized light-induced anisotropy [5–8]. For comparison, the UV–Vis spectrum of AZO-1 in dilute solution is also included as Fig. 2(b). The absorption maximum (λ_{max}) of AZO-1 doped PMMA film is red shifted by 20 nm (490 nm) in comparison to that in dilute solution (470 nm), indicating the J-aggregation of azobenzene chromophores in polymer film [18]. It can be seen that the film has a little absorbance at around 633 nm. This makes it possible to record

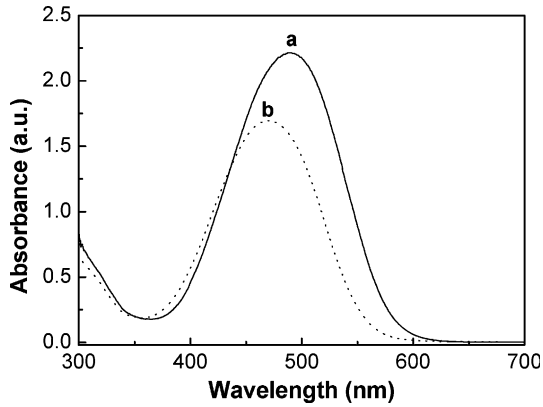

Fig. 2. UV–Vis spectra of AZO-1 doped in PMMA with the concentration of 1 wt% (a) and in $CHCl_3$ with the concentration of 0.01 mg/ml (b).

holographic gratings in the polymer film upon exposure to an interference pattern of two beams from He–Ne laser of 632.8 nm.

3. Formation of holographic gratings

Measurements of diffractive signals of transmission holograms are carried out using the system described in Fig. 3. At this moment, Nd:YAG laser is turned off. The holographic recording is accomplished by two linearly polarized beams from He–Ne laser of 632.8 nm and the polarization directions are controlled by half-wave plates. The diameter of the laser point is about 0.15 cm. The intersecting angle between the two beams is set to be about 10°. Each beam acts both as a writing beam to write the grating and a reading beam to read the grating [15]. The first and second order diffraction can be observed clearly. Since I_1^+ and I_1^- are in the directions of recording beams, they cannot be used to monitor the recording of the holographic grating. While I_2^+ and I_2^- cannot monitor the decay of the grating because they fall rapidly as one of recording beam is shut off. The diffractive signals are received by a charge-coupled device (CCD, sensitive region from 350 to 900 nm) and transferred to a computer directly.

Fig. 4(A) shows the second-order diffractive signal of the holographic gratings recorded by two He–Ne beams in the same (p, p and s, s) or different (p, s) polarization with a fixed power $P = 4$ mW (power density is 4/0.07 mW/cm^2) of each

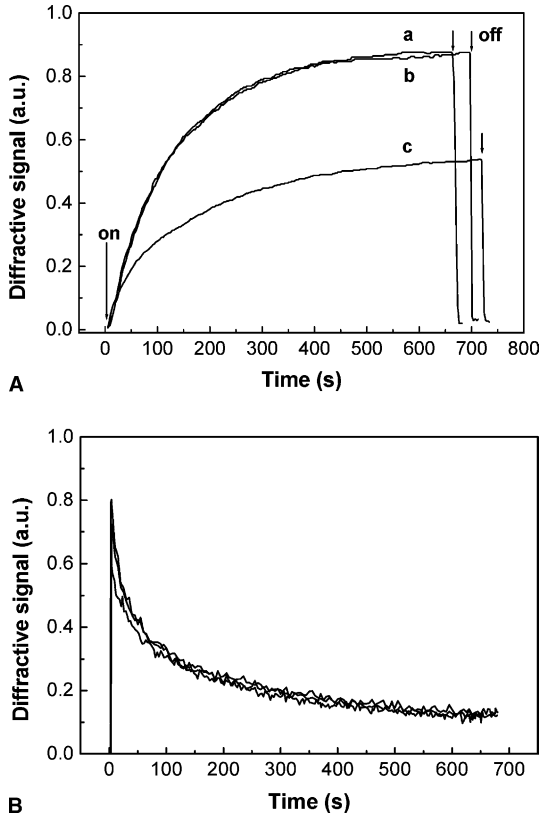

Fig. 4. (A) The growing processes of the second-order diffractive signal of the holographic gratings recorded by two He–Ne beams with a fixed power density of 4/0.07 mW/cm^2 of each beam: (a) p, p grating, (b) p, s grating, (c) s, s grating. (B) The decay processes of the first-order diffractive signal of the holographic gratings recorded by two He–Ne beams in the same (p, p or s, s) or different (p, s) polarization with a fixed power density of 4/0.07 mW/cm^2 of each beam.

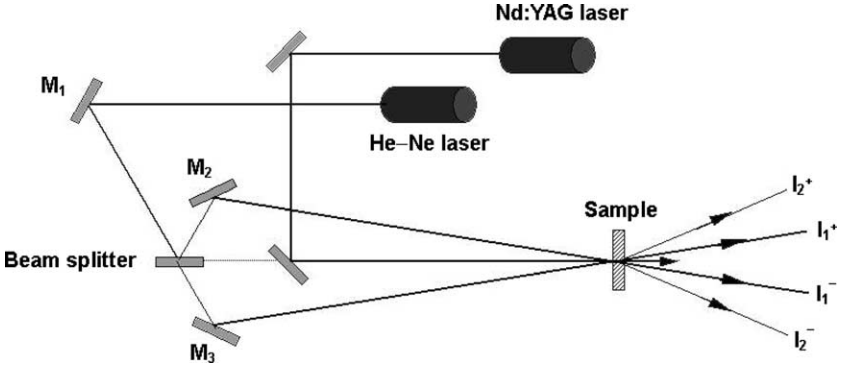

Fig. 3. The experimental setup for the formation of holographic gratings. I_1^+, I_1^- and I_2^+, I_2^- are the first-order and second-order diffractive beams, respectively.

writing beam. Two processes take place when the sample is irradiated by He–Ne laser. One is the formation of *cis*-isomers due to light absorption of the azo-chromophores and the other is reorientation of azo-chromophores accompanied by the optically induced anisotropy. The diffractive signals from the photoinduced gratings are resulted in sum of phase change through the dye-doped polymer film. The moments of turning on and off the recording light are marked by the arrows in Fig. 4(A). The recording of holographic grating is rather slow since the absorption of the AZO-1 at 633 nm is very weak. The diffractive signals increase slowly and reach the saturated value after turning on the recording light for about 500 s. The diffractive signals of the recorded gratings are dependent on the polarization direction of the recording beams. It is demonstrated that the diffractive signals of p, p-grating and p, s-grating are similar to each other and that of s, s-grating is much smaller than the formers. The overall change in the diffractive signal is normalized between 0 and 1 for the sake of clarity of presentation. When one of the recording beams is turned off, the intensity of the signal falls rapidly. Fig. 4(B) shows the decay processes of the first-order diffractive signals of the holographic gratings recorded by two He–Ne beams in the same (p, p or s, s) or different (p, s) polarization with a fixed power density of 4/0.07 mW/cm^2 of each recording beam. There are no obvious differences between these decay processes and they reach the same steady value eventually.

To investigate the dependence of diffractive signals on the power density of recording beams, two series of experiments are carried out. Firstly, one of the recording beams (I_1) is set to be 4/0.07 mW/cm^2 and the other beam (I_2) is varied from 1/0.07 to 10/0.07 mW/cm^2. Fig. 5(a) shows the plots of the maximum of the diffractive signals vs the power density of beam I_2 when beam I_1 is fixed at 4/0.07 mW/cm^2. It can be seen clearly that both the first-order and second-order diffractive signals increase with the enhancement of beam I_2. This increase is resulted by two factors that including the increase of diffraction efficiency of the grating and the coupling of the two writing beam [15]. Secondly, the total power density of beam I_1 and

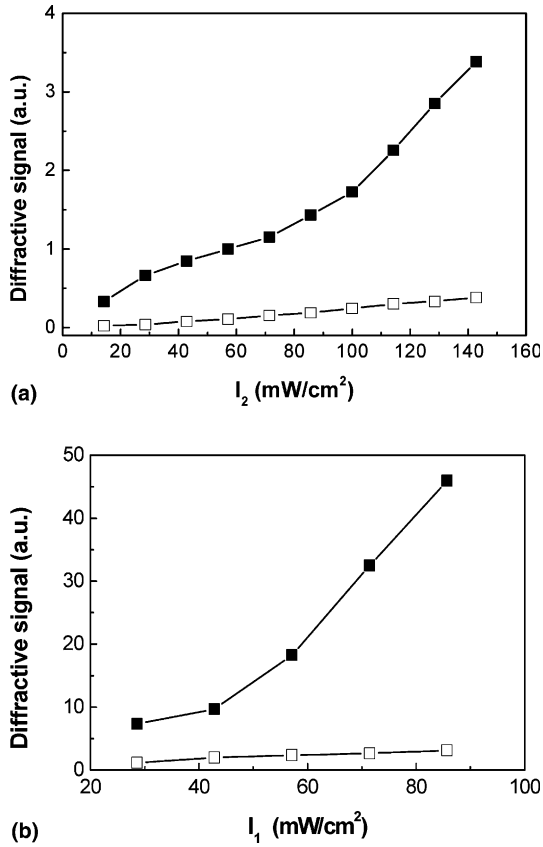

Fig. 5. (a) The plots of the maximum of the diffractive signals vs the power density of beam I_2 when beam I_1 is fixed at 4/0.07 mW/cm^2. (b) The plots of the maximum of the diffractive signal vs the power density of beam I_1 when the total power of I_1 and I_2 is fixed at 12 mW. The solid squares represent the first-order diffractive signals and the hollow squares represent the second-order diffractive signals.

beam I_2 is fixed at 12/0.07 mW/cm^2 and the dependences of the diffractive signals on the power density are shown in Fig. 5(b). The diffractive signals increase with the reducing of the difference between the two beams in intensity. The diffractive signals reach the maximum when the beam ratio is set to be 1.0.

4. Formation of holographic gratings accompanied by 532 nm irradiation

The formation of holographic grating accompanied by 532 nm irradiation is carried out using

the system shown in Fig. 3. The holographic recording is accomplished by two linearly polarized He–Ne laser of 632.8 nm with the same polarization and the power density of each beam is 4/0.07 mW/cm^2. The experiments are accomplished as follows: the 532 nm laser and two He–Ne beams are switched on at the same time; after the second-order diffractive signal reaches a saturated value, 532 nm laser is switched off; when the second-order diffractive signal reaches another saturated value, one He–Ne beam is switched off. These three steps are indicated as *a*, *b*, and *c* in Fig. 6(A).

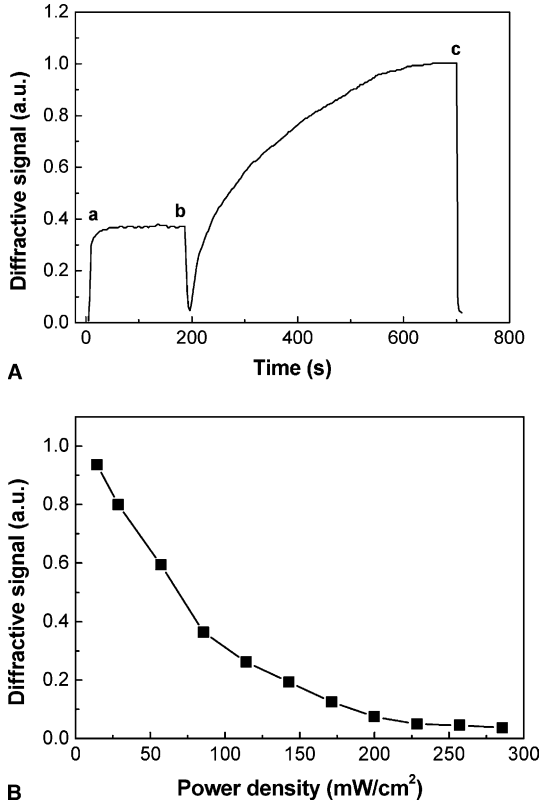

Fig. 6. (A) The second-order diffractive signal of He–Ne beam through the holographic grating: (a) the 532 nm laser and two He–Ne beams are switched on at the same time; (b) the 532 nm laser is switched off; (c) one He–Ne beam is switched off. The power density of 532 nm laser is 6/0.07 mW/cm^2 and each He–Ne beam is 4/0.07 mW/cm^2. (B) The plot of the maximum of the diffractive signal between step *a* and *b* vs the power density of 532 nm laser. The overall change of the diffractive signals is normalized by taking the value at point *c* as 1.0.

When 532 nm laser and two He–Ne beams are switched on at point *a*, the diffractive signal increases rapidly and reaches a steady value after a few seconds. On turning off 532 nm laser, the diffractive signal drops almost to zero, and then rise up again. AZO-1 doped polymer film has strong absorbance at around 532 nm as shown in Fig. 2. 532 nm laser can induce a rapid *trans–cis* isomerization of AZO-1 and a balance between the *trans*-isomer and the *cis*-isomer is built. In this background, the formation of the holographic grating induced by the two interferential He–Ne beams is accelerated. When 532 nm laser is turned off, most of the *cis* isomers formed via the photoisomerization process thermally reisomerize to the *trans* molecule quickly as discussed in Section 2. So the diffractive signal falls rapidly almost to zero and after that the two He–Ne beams begin to write a holographic grating again. The diffractive signal reaches a saturated value after about 500 s. On the other hand, 532 nm laser has a tendency to erase the holographic grating formed by two He–Ne beams. This maybe leads to the decrease of the diffractive signal. The diffractive signal between step *a* and step *b* is the result of the synergetic effect of the two factors mentioned above.

To investigate the dependence of the diffractive signals on the laser intensities, the power density of 532 nm laser are varied from 1/0.07 to 20/0.07 mW/cm^2. Fig. 6(B) is the plot of the maximum of the second-order diffractive signal between step *a* and *b* vs the power density of 532 nm laser. The overall change of the diffractive signals is normalized by taking the value at point *c* as 1.0. The acceleration effect of 532 nm laser to the formation of holographic grating is predominant when the power density of 532 nm laser is low. While at relatively high intensities of 532 nm laser, the erasure is the main factor to the holographic grating. For example, the diffractive signal is 0.936 at 1/0.07 mW/cm^2 of 532 nm laser; while at 20/0.07 mW/cm^2 the diffractive signal is only 0.037. For all the power density of 532 nm laser, the diffractive signals after step *b* are similar to each other. They reach the same saturated value as shown in Fig. 6(A).

Since the erasure of 532 nm laser at low power density is the minor factor to the holographic

grating, it is possible to probe the holographic grating induced by two He–Ne beams using 532 nm laser. Fig. 7(a) is the first-order diffractive signal of 532 nm laser through a grating written by two He–Ne laser beams. The power density of 532 nm laser is 1/0.07 mW/cm^2 and each He–Ne beam is 4/0.07 mW/cm^2. When 532 nm laser monitors the holographic grating, its acceleration effect is unavoidable. Fig. 7(b) shows the dependence of first-order diffractive signal of the holographic grating on the power density of He–Ne laser beams. The He–Ne laser beam ratio is set to be 1.0. The diffractive signal increases with the recording power density. When the hologram is erased, it can be rewritten and the same value of diffraction efficiency can be achieved after multiple uses.

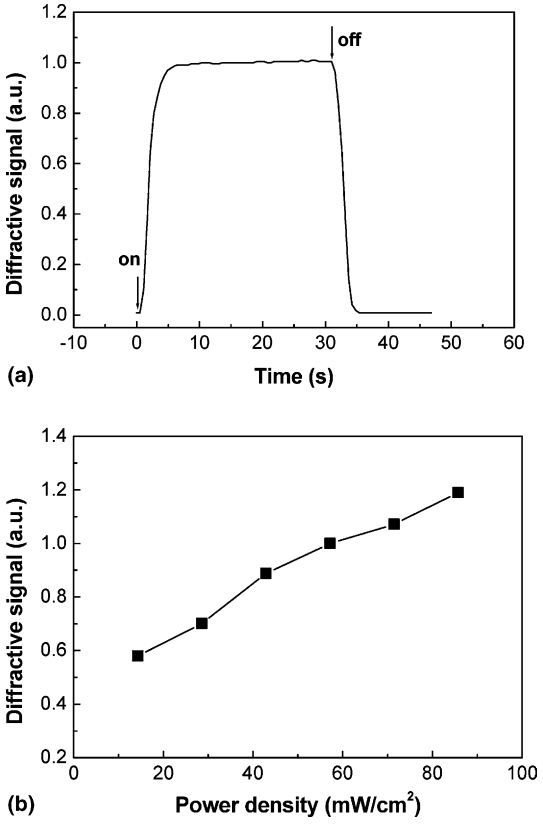

Fig. 7. (a) The first-order diffractive signal of 532 nm laser through a grating written by two He–Ne beams. The power density of 532 nm laser is 1/0.07 mW/cm^2 and each He–Ne beam is 4/0.07 mW/cm^2. (b) The dependence of first-order diffractive signal of the holographic grating on the power density of He–Ne beams. The He–Ne beam ratio is set to be 1.0.

5. Summary

Holographic gratings were recorded by He–Ne laser of 632.8 nm in PMMA film containing push–pull azo dye. The holographic characteristics of the recorded gratings were related to the polarization direction and intensities of the recording beams. The studies of the holographic gratings accompanied by 532 nm irradiation indicated that 532 nm laser played an important role in the formation of the holographic grating. The holographic grating recorded was the result of the synergetic action of the acceleration effect and the erasure of 532 nm laser to the grating. The holographic grating was probed by 532 nm laser and the diffractive signal increased with the power density of recording beams. The azo dye doped polymer film allowed multiple uses without apparent fatigue.

Acknowledgements

This work was supported by the National Natural Science Foundation of China, the program of CAS Hundred Talents, Excellent Young Teacher Foundation of Ministry of Education of China, and the Jilin Distinguished Young Scholar Program.

References

[1] J.A. Delaire, K. Nakatani, Chem. Rev. 100 (2000) 1817.
[2] G.S. Kumar, D.C. Neckers, Chem. Rev. 89 (1989) 1915.
[3] Y. Atassi, J.A. Delaire, K. Nakatani, J. Phys. Chem. 99 (1995) 16320.
[4] S. Houbrechts, K. Clays, A. Persoons, Z. Prikamenou, J.-M. Lehn, Chem. Phys. Lett. 258 (1996) 485.
[5] P.-A. Blanche, Ph.C. Lemaire, C. Maertens, P. Dubois, R. Jérôme, Opt. Commun. 139 (1997) 92.
[6] P. Lefin, C. Fiorini, J.-M. Nunzi, Opt. Mater. 9 (1998) 323.
[7] K. Tawa, K. Kamada, K. Ohta, J. Photochem. Photobio. A 134 (2000) 185.
[8] H. Ono, N. Kowatari, N. Kawatsuki, Opt. Mater. 17 (2001) 387.

[9] K. Munakata, K. Harada, M. Itoh, S. Umegaki, T. Yatagai, Opt. Commun. 191 (2001) 15.
[10] C.R. Mendonça, D.S. Dos Santos Jr., D.T. Balogh, A. Dhanabalan, J.A. Giacometti, S.C. Zilio, O.N. Oliveira Jr., Polymer 42 (2001) 6539.
[11] L.M. Blinov, G. Cipparrone, M.V. Kozlovsky, V.V. Lazarev, N. Scaramuzza, Opt. Commun. 173 (2000) 137.
[12] C. Wang, H. Fei, Y. Yang, Z. Wei, Y. Qiu, Y. Chen, Opt. Commmu. 159 (1999) 58.
[13] D.S. DosSantos Jr., C.R. Mendonça, D.T. Balogh, A. Dhanabalan, A. Cavalli, L. Misoguti, J.A. Giacometti, S.C. Zilio, O.N. Oliveira Jr., Chem. Phys. Lett. 317 (2000) 1.
[14] L.M. Blinov, M.V. Kozlovsky, G. Cipparrone, Chem. Phys. 245 (1999) 473.
[15] X. Wei, X.Z. Yan, D.R. Zhu, D. Mo, Z.X. Liang, W.Z. Lin, Appl. Phys. Lett. 68 (1996) 1913.
[16] Y. Liu, H. Wang, M. Tian, J. Lin, X. Kong, S. Huang, J. Yu, Opt. Lett. 20 (1995) 1495.
[17] H. Fei, Z. Wei, P. Wu, L. Han, Y. Zhao, Y. Che, Opt. Lett. 19 (1994) 411.
[18] H. Menzel, B. Weichart, A. Schmidt, S. Paul, W. Knoll, J. Stumpe, T. Fischer, Langmuir 10 (1994) 1926.